ANISOTROPIC ETCHING OF p-Si IN HF SOLUTION[*]

R. Outemzabet[a]**, N. Benzekour, N. Gabouze**[1]**, N. Kesri**[a]**, K. Ait-Hamouda**
UDTS, 2 Bd Frantz-Fanon, B.P. 399 Alger-Gare, Algiers, Algeria
[a] *USTHB, département de physique, Algiers, Algeria*

In situ electrochemical attenuated total reflection Fourier transform infrared (ATR-FTIR) spectroscopy has been used to study the etching process on a Si (100), (110) and (111) surface in dilute HF solution. On the other hand I-V characteristic of the p-Si-HF system was used for the interface reactions and kinetics study. Infrared results show that monohydride (SiH) and hydroxyl (Si-OH) species surface concentration depend on the applied potential to the electrode. I-V characteristics show a relative variation in magnitude of the first peak as the substrate orientation is changed. A mechanism of silicon dissolution is proposed.

1 Introduction

The electrochemical etching of silicon in fluoride containing electrolytes is of interest because of the possibility of etching 3 - dimensional structures (optics, sensors. . . .). A variety of morphologies can be produced depending upon the type of silicon substrate and the preparation conditions. Several papers were published dealing with pores on p-type Si and their possible formation mechanism, but the dependence of pore morphologies on crystal orientation was neither studied very much nor well understood [1]. The dependence of macropore morphology on the orientation of p- and n-type silicon samples was studied for various organic and aqueous electrolytes containing hydrofluoric acid by Christophersen et al. [2]. The results show that the macropore formation in p-and n-type silicon is a strongly anisotropic process. Depending on the substrate orientation <100> and <113> preferred growth directions could be observed. Lehmann already found that macropores tend to grow in <100> directions [3]. Propst and Kohl found that a certain indirect orientation dependence for p-type was also found for macropores in p-type Si obtained in water-free MeCN, because no pores could be obtained on {111} –oriented surfaces in contrast to (100) surfaces [4]. Lehmann [3] regarded as very plausible that the anisotropy of the electropolishing current bears the explanation for the anisotropy of pore shape and pore growth direction. On the other hand, Föll et al. [5] have proposed a new model to explain the anisotropic pore growth. At the core of the model is the idea of a competition between oxidation and hydrogenation, a competition that would lead to unstable behavior on a local scale. When the oxide gets thick enough, the current vanishes, the oxide dissolves, and the surface gets rehydrogenated and passivated, till a new cycle starts. The hydrogen repassivation step would be that responsible for
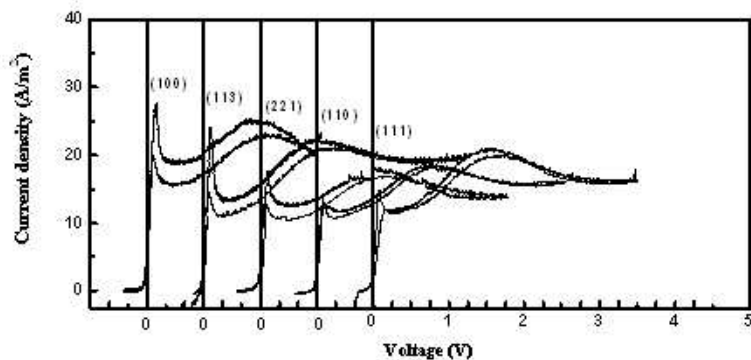
Fig. 1. Cyclic voltammograms of p-Si with different crystal orientations showing the characteristic peaks (J_1, J_2, J_3 and J_4). C_F = 0.1 M, pH = 3, scan rate = 5mV/sec.
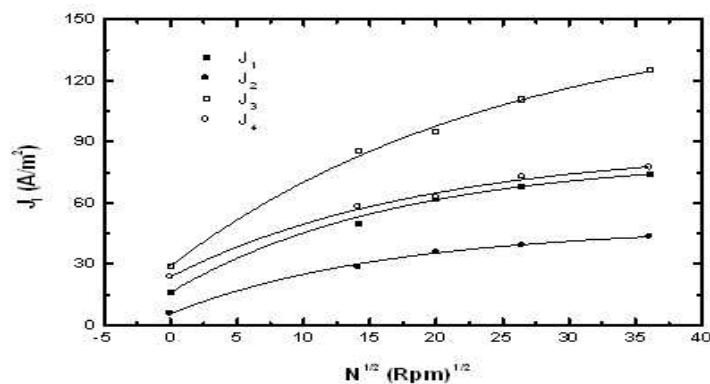
Fig. 2. Current densities as a function of the rotation for p-Si (110). $C_{F=}$0.05 M, pH = 3.

the anisotropic effects. However, anisotropy of the electropolishing current may also result from factors not taken into account in Föll's model (e. g., role of SiOH species), and the oscillatory nature of the current on the microscopic scale does not appear as mandatory requirement for electropolishing to take place. Therefore, we need an understanding of the microscopic etching process of silicon electrode surfaces during anodization in etching solution, in order to control the structure of porous Si.

In the present paper, we have investigated in-situ during anodization the etching process on p-Si(100), (111) and (110) electrode surface in dilute HF solution, using infrared spectroscopy. On the order hand I-V characteristic of the p-Si –HF system was used for the interface reactions

and kinetics study.
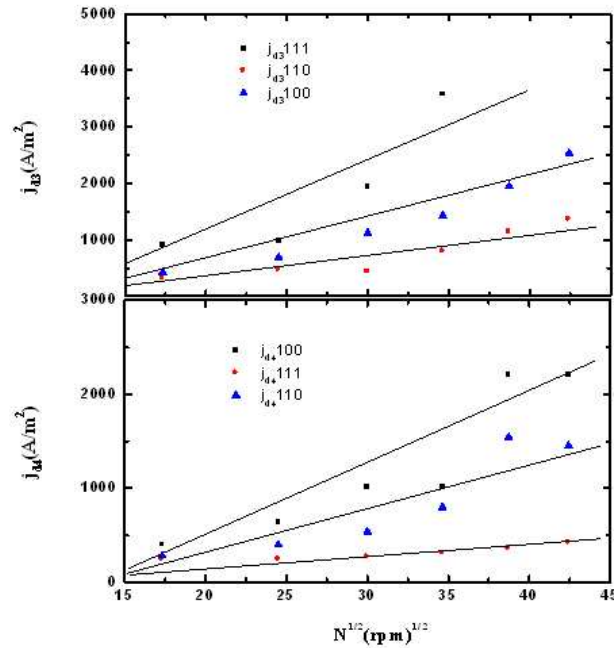
Fig. 3. Diffusion current-density $j_{d3,4}$ determined from the measured current density j at different rotation rate of p-Si ((100), (110), (111)) electrode and from the true kinetic current density j_k for $C_F = 0.2$ M, pH = 1.

2 Experimental

The samples were prepared from p-Si single crystals, double-side polished, of different orientations (100), (111), (110). Samples were 0.4 mm thick and (110) oriented sample was 1 mm thick with resistivity in the range $0.01 \div 0.1$ Ωm. They were back contacted using Au- (1%) Al vacuum deposition at 600 ˚ c. They were first shaped into disk with 4 mm diameter (by mechanical polishing) and then mounted and fixed on the mass rod of the rotative disk electrode system with silver epoxy. (The rod was shaped to provide back electric contact. It was sealed with epoxy resin into a Plexiglas cylinder). Since the experiments and interpretation are complicated by the formation of H_2 gas bubbles on the electrode surface, we use a common face-down rotating disk electrode. The other crystal orientations were produced by cutting slices from Si crystal end piece at predetermined orientations. The realisation of controlled mass-transport conditions at the interface has been found to be critical in obtaining highly reproducible voltammograms; the solutions used
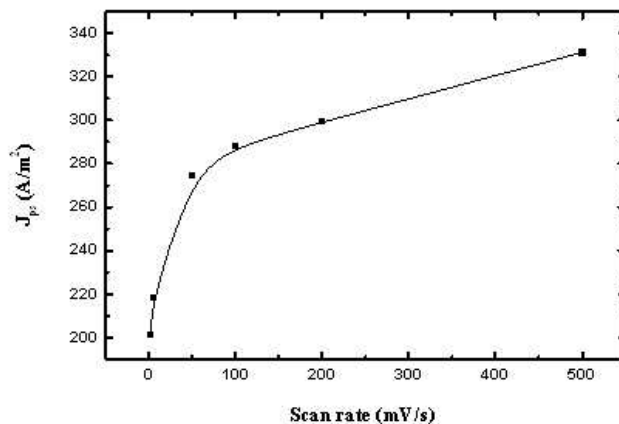
Fig. 4. Current density (J_{PS}) of p-Si (100 in 5% HF as a function of the scan rate.

were prepared from water deionised by a millipore system (mini Q), The electrolytes were prepared from deionised water, ammonium fluoride and hydrofluoric acid. For C_F <1 M, the ionic strength of the solution was kept to 1M by adding ammonium chlorides. For example, a typical solution was $0.05 M NH_4F + 0.05 M HF + 0.9 M NH_4Cl(C_F = 0.1M, pH = 3)$. The electrode was rotated from 50 to 3000 r.p.m. For each solution, the pH was verified using coloured indicators and pH-meter. The native oxide was removed by immersing samples in 5% HF. The electrochemical set-up consisted of a polystyrene cell and a classical three electrode arrangement, including a rotating Si disk as working electrode, an Ag/AgCl (in satured KCl) reference, and a Pt-wire counter electrode. The current potential curves were controlled by a potentiostat. The infrared analysis was performed in ATR mode with ten useful reflections at the electrochemical interface using a Bomen MB100 Fourier Transformer Spectrometer in-situ. In-situ spectra were recorded at several potentials during the anodic dissolution of the p-Si samples.

3   Results

3.1   I-V polarization curves

We have collected in Fig. 1 the voltammograms obtained for (100), (111), (110), (113) and (221) – oriented Si surfaces in the same electrolyte (C_F = 0.1 M). The overall shape of all these voltammograms is rather similar: when the electrode potential V is swept toward positive values, one observes first a steep current rise near 0V, followed by a sharp peak and a narrow plateau. The rising part of the voltammogram, near 0V is known to be associated with the generation of porous silicon (PS). The presence of the first current peak (J_1) at the I-V curves has always been considered as a frontier between the PS growth and electropolishing. This peak does not repre-
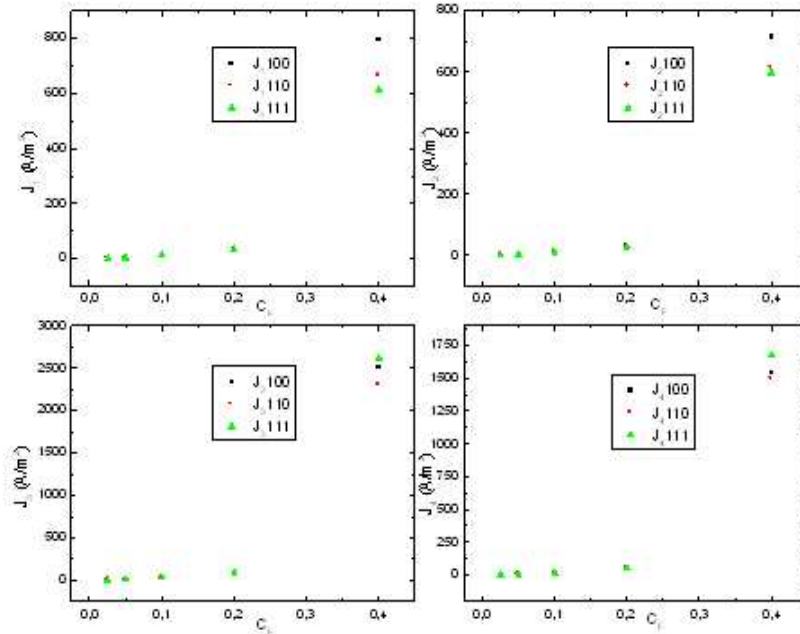
Fig. 5. Dependence of the current densities J_1, J_2, J_3 and J_4 with the concentration C_F for different crystal orientation. Si (0.01 Ωm) rotation rate = 300 r. p. m. potential sweep = 5 mV/sec.

sent qualitative changes in the balance of electrochemical reactions but is rather a consequence of morphological changes tacking place in the system. Then a second broad maximum (J_3) is found in the range + 1 to 2.5 V [6]. Beyond the potential of the second maximum, the current decreases and reaches a plateau (J_4); such a behaviour is usually interpreted as the appearance of a steady state in which the current is limited by the chemical dissolution of an electrochemically produced oxide layer. In the range V>1 V, the I(V) are independent of the electrode orientation [6]. A most striking feature is the relative variation in magnitude of the first peak as the substrate orientation is changed. J_{ps} is largest for silicon electrodes of <100> crystal orientation and is independent of the electrolyte concentration used as determined by Lehmann [3]. This independence indicates that the dissolution process is of anisotropic nature.

When electrode rotation is used, these curves are found to be reproducible for a given solution. The dependence of the voltammograms upon electrode rotation rate has been investigated and it is shown that the rotation of the electrode influences the current-potential significantly. From voltammograms recorded at different rotation rates (for C_F = 0.05 M and pH = 3, N vary from 0 to 1800 r.p.m.) we plotted in Fig.2 the currents $J_1, J_2, J_3,$ and J_4 as a function of the square root of the rotation rate. One can note that the variation in current for rotation speeds higher than
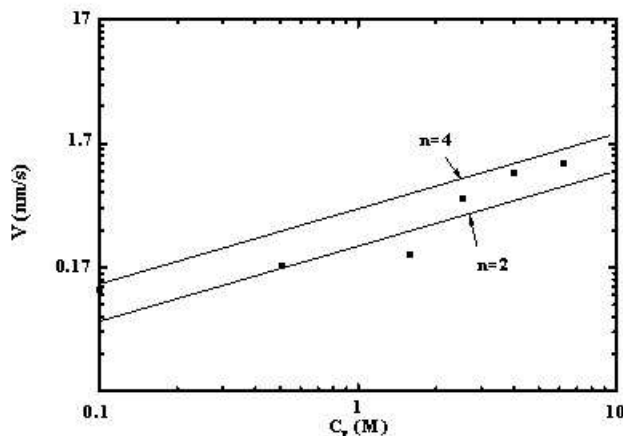
Fig. 6. Growth rates of pores (V) calculated from Eq. 1 plotted for n = 2 and n = 4 (lines) and experimentally obtained growth rates (square) vs. the HF concentration (C) of the electrolyte.

300 r.p.m. was not very great. At higher C_F, the effect of the rotation rate on the current was more significant). It was found that for these current densities the Levich relation is not obeyed. This result means that mass transport is not the only rate limiting process in the anodic dissolution of Si as concluded by Memming and Schwandt [7]. The experimental results were analysed in order to obtain the extrapolation of the measured current to infinite angular velocity of the rotating electrode. This has been done by an analyse of the currents using a simple Koutecky –Levich equation [8]:

$$\frac{1}{J} = \frac{1}{J_k} + \frac{1}{J_d} \tag{1}$$

Where J, j_k and $J_d \alpha N^{1/2}$ are the measured, the kinetic and the diffusion current densities, respectively. When the four currents are represented in terms of J^{-1} as a function of $N^{-1/2}$ we found linear plots. The inverse of the extrapolated value at $N^{-1/2} = 0$, which correspond to infinite rotation rate, is in each case the true kinetic current, J_k, which is potential dependent. J_k corresponds to a situation in which the surface and bulk concentrations are identical. The striking identical slope of the straight lines obtained suggests that the diffusion limitation is due to the same species over the whole potential range [9]. In a representation of J_d as a function of the square root of rotation rate a linear relationship going through the origin is obtained. These plots are presented in Fig. 3 for solution of pH = 1 with C_F = 0.2 M. From such plots, more detailed information about the diffusing species could probably be obtained from the dependence of $J_d N^{-1/2}$ on C_F and pH. From the true kinetic current in each case it would be possible in principal to calculate the kinetic parameters of the system studied. The influence of temperature, HF concentration and rotation rate on the photo-anodic dissolution of a n-type Si rotating disk
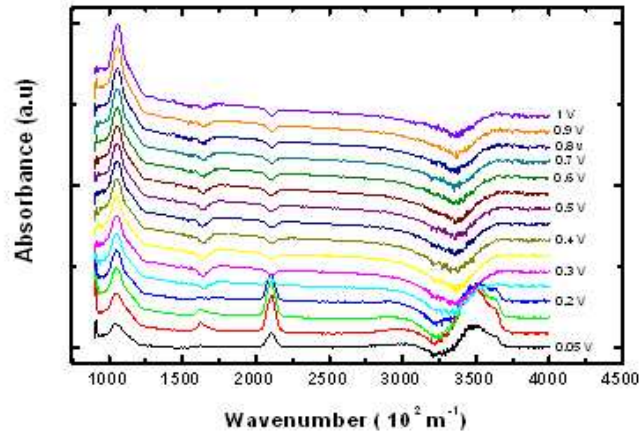
Fig. 7. IR absorbance spectra as a function of potential of a (100) p-type silicon sample in the anodic scan. C_F=0.05 M.

electrode in water/ethanol/HF solution has been investigated by van den Meerakker et al. [10] It has been found that the first peak current was under mixed kinetic/diffusion control. An other striking feature is the relative variation in magnitude of the first peak as the scanning rate is varied. The I-V characteristic obtained (100) oriented Si surfaces in C_F = 5% at different scan rate, shows an increase of the first peak with the increase of the scan rate. The current J_1 increases in a logarithmic manner with $N_{sr}^{1/2}$(Fig. 4).

We have determined for the three crystallographic orientations (100), (110) and (111), the evolution with the concentration of F, which is shown in Fig. 5. At first analyse it may be seen that all the currents for the three orientations increase with increasing C_F. The variation is of the type J α C_F^2, which is consistent with ref. 11. The authors reported that in the higher C_F range and for low pH values, the dependence of J_2 is slightly attenuated, a point which has already been noticed by Eddowes [12]. It is interesting to notice that for C_F = 0.4 M, $J_1(100) > J_1(110) > J_1(111)$ and $J_3(111) > J_3(100) > J_3(110)$. However, for the current J_4 that corresponds to the electropolishing regime, we found J_4 (100) $\approx J_4$ (110), which indicates that oxidation of silicon occurs in the same manner on (100) and (110) surface. For J_2 which corresponds also to the electropolishing regime, J_2 (110) $\approx J_2$ (111). The current densities J_1 and J_3 can be converted into etch rates, assuming four elementary charges per dissolved silicon atom. The current density at the electrode surfaces is a measure of the rate of dissolution. Consequently the rate of pore growth can be calculated if the local current density at the pore tip J_{tip} is divided by the dissolution valence n (number of charge carriers per dissolved silicon atom), the elementary
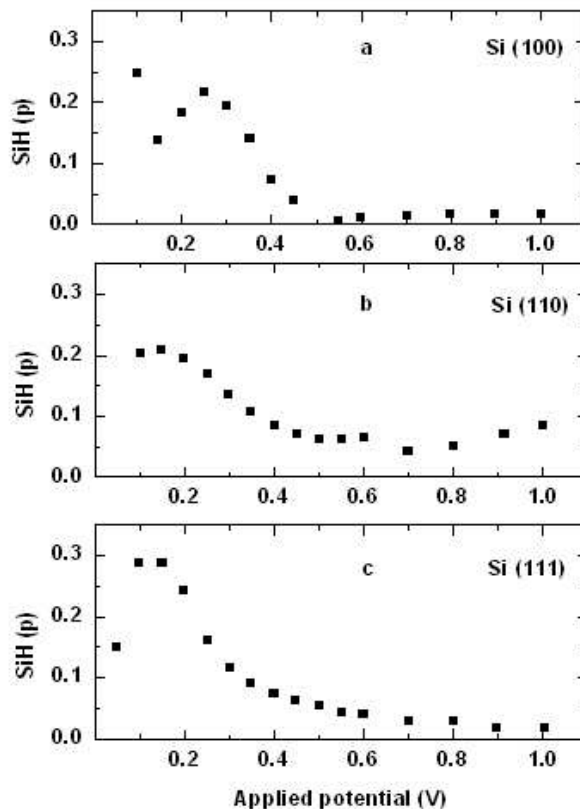
Fig. 8. Integrated infrared absorbances of the Si-H stretching vibrations at 21×10^4 m^{-1} as a function of applied potential of p-Si (100) . $C_F = 0.05$ M, pH = 3.

charge e (1.602×10^{-19} C), and the atomic density of silicon N_{si} (5×10^{28}/m^3).

$$V = \frac{J_{tip}}{n(-e)N_{Si}} \tag{2}$$

It is assumed that for stable pore growth, which occurs when the current density is limited by hole generation and not by the applied bias, J_{tip} is equal to the critical current density J_{ps}. For $J > J_{ps}$, holes accumulate at the electrode surface, and HF is depleted at the electrode surface. Consequently dissolution is limited by the mass-transfer rate that is lower in depressions or pits, which results in electropolishing of the surface. For $J < J_{ps}$, the reverse is true: holes are depleted at the electrode, and HF accumulates at the electrode surface. Therefore every depression or pit
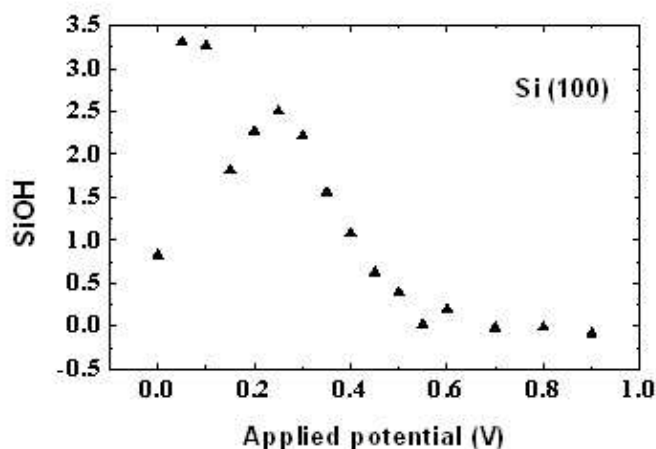
Fig. 9. Integrated infrared absorbances of the Si-OH stretching vibrations at 34×10^4 m^{-1} as a function of applied potential of p-Si (100). $C_F = 0.05$ M, pH = 3.

in the surface initiates pore growth because it focuses the electric field lines of the space-charge region and thereby enhances the local current density. At $J = J_{ps}$, ionic transfer and charge supply are in a steady–state condition. The dissolution valence increases with current density from a value of 2 to 4 [3]. The figure 6 shows that the experimentally observed growth rates plotted as a function of the HF concentration and crystal orientation fit well with the calculated values of V for n = 2 and n = 4 (lines in Fig. 6). The results suggest that n varies depending on the formation conditions. Experimentally we found V = 1.08 nm/s. for the <100> direction and V = 0.87 nm/s. for the <113> direction. This means that for a given current and pore diameter, the pore growth velocity is 1.08/0.87 = 1.25 times faster in the <100> direction compared to <113> direction, value close to that observed by Föll et al. [13].

3.2   Infrared absorption measurements and analysis

IR absorption in internal-reflection geometric is a suitable technique for the study of the silicon/electrolyte interface, allowing to in situ follow the evolution of the chemistry of the silicon surface as a function of the electrochemical treatment. It is known that simple rinsing of silicon in fluoride media may lead to atomically flat surfaces, as well as rough surfaces [14,15]. We applied positive potentials ranging from 0 to 1 V to the Si electrode and monitored spectral changes in the Si-OH and Si-H stretching vibration region. Fig. 7 shows the absorbance spectra at several selected potentials, for silicon in the $C_F = 0.05$ M, pH = 3 electrolyte. In the range (0 – 0.25 V) corresponding to the steep current rise regime, the build up of a hydrogenated surface of high specific surface area can be confirmed by the appearance of a SiH absorption near 21×10^4 m^{-1}.
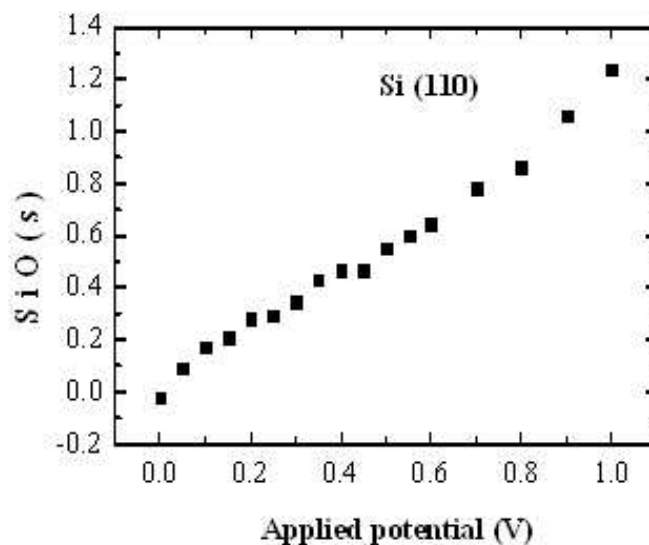
Fig. 10. Integrated infrared absorbances of the Si-O stretching vibrations at 10.6 x 10^4 m^{-1} as a function of applied potential of p-Si (110). $C_F = 0.05$ M, pH = 3.

Si(100)

When a positive potential was applied to the electrode monohydride (SiH) species increased its surface concentration reaches a maximum concentration at about 0.10 V and then decreased (Fig. 8a). At potentials positive of this first current peak the Si-H bonds are lost and new Si-O bonds appear, shown by two absorption bonds at around 10.6 x 10^4 m^{-1}, which is assigned to the asymmetric Si-O-Si vibration mode. The increase of the oxide absorbance bands observed in Fig. 7 is accompanied by an increase of the negative contributions at 16.5 x 10^4 and 34 x 10^4 m^{-1}, ascribed to H_2O. When an oxide layer of a certain volume is formed, it replaces the same electrolyte volume near the interface, hence electrolyte absorption in the probed region becomes weaker than in the reference non oxidized state. The oxide layer induces a shielding effect of the electrolyte absorption [16]. The Si (100) electrode surface was initially terminated by dihydride species (SiH_2). At early stages of etching dihydride species on the topmost layer of the electrode surface are removed, thereby producing monohydride on the second layer [17]. Fig. 9 Reveals that the Si-OH species increases its concentration reach a maximum at 0.1 V, then decrease to a minimum at 0.15 V and reach a maximum at 0.25 V to decrease in an exponentially manner with the applied potential. The minimum of the Si-OH concentration species corresponds to the maximum concentration of Si-H species on (110) and (111) Si surface.

Fig. 11. Mechanisms of silicon dissolution in HF electrolyte.

Si (110)

On the starting Si (110) surface, monohydride species is a dominant hydride species increases its concentration, reaches a maximum at about 0.15 V and stabilize at around 0.5 – 0.7 V (Fig. 8b). An increase of monohydride species is observed at potential above 0.8 V; Niwano has shown that the decrease of SiH species is accompanied by the increase of SiH_2 species and interpreted that removal of monohydride species on the topmost layer produces dihydride species and monohydride species on the second layer of the surface [17]. As can seen from Figs.8, when the applied potential is increased (above 0.15 V), the hydride modes, Si-H and $Si-H_2$, decreased in intensity, which indicates that surface Si-H bonds are attacked by oxygen to be converted to the Si-O bonds. As shown in Fig. 10, the SiO increase continuously with the applied potential. The same behavior is obtained for the (100) and (111) surface.

Si (111)

When a positive potential was applied to the Si(111) electrode, monohydride species increased its surface concentration, reaches a maximum at 0.15 V and then decreases in an exponentially manner with the applied potential as shown in Fig. 8c. One can observe from Figure 8c that potential corresponding to the maximum surface concentration of the monohydride species is located at 0.10 V for Si (100), and 0.15 V for (110) and (111) Si surface. This result means that probably Si (100) surface is first dissolved, confirming the anisotropy. An interesting

phenomenon is that the band obtained in-situ is considerably broader than that from ex-situ IR investigation mainly due to the interaction between terminal hydrides with water molecules [18]. When a positive potential was applied to the electrode monohydride (SiH) species surface concentration is found to be the same for (100) Si and (110) Si surface. At 0.1 V, the (100) Si surface is more covered by the SiH that the (110) Si surface. At 0.15 V, the (100) Si surface decreased its SiH species, while the (110) Si surface increased its surface concentration.

3.3   Mechanism of silicon dissolution

Silicon is probably the only semiconductor that spontaneously give rise to well defined pores with nm dimensions. The interaction of hydrogen with semioncductor surfaces is the subject of intense investigation, since the formation and breaking of Si-H bonds are believed to be rate determining in chemical processes on the Si surface. Based on the results presented above, we consider the mechanism of wet oxidation, we suppose that the following steps are involved in the wet oxidation.

In a solution of lower pH, the hydrogenated surface might directly change into a surface terminated by hydroxyl [19]. It was reported that OH^- is involved in the chemical etching of silicon in HF or NH_4F. By analysing the change in the intensity of the two bands at 21 x 10^4 m^{-1} and 34 x 10^4 m^{-1}, one type is that OH^- ions or H_2O directly attack and replace the sites of hydrogen (a b) , Fig.11, followed by several similar processes (b c), leading to the decrease of the intensity of the band centred at 21 x 10^4 m^{-1}. These oxidation processes may dominate on the hydrogen desorption in the lower pH. As has been previously pointed out OH^- ions may be involved in the oxidation of Si crystal surfaces [20]. We therefore excepted that the rate of oxidation depends on the pH of the etching solution. As shown, with increasing pH, F^- containing species may bond (b d) to the surface together with the OH^- ion. This lead to a more easy insertion of O into the Si-Si bond with the contribution of the F atom of large electronegativity (d e f).

4   Conclusion

The electrochemical etching of p-Si (100), (111) and (110) electrode surfaces in dilute HF solution has been investigated by using in situ electrochemical ATR-FTIR spectroscopy. It was found that Si-H and Si-OH species surface concentration depend on the applied potential. The maximum concentration of species corresponds to the potential of the first peak on I-V characteristics. It depends on crystal orientations. In addition a relative variation in magnitude of the first peak as the substrate orientation is changed has been shown.

References

[1] S. Rönnebeck, J. Carstensen, S. Ottow, H. Föll: Electrochem. Solid-State Lett. **2** (1999) 126

[2] M. Christophersen, J. Carstensen, S. Rönnebeck, C. Jäger, W. Jäger, H. Föll: J. Electrochem. Soc. **148** (2001) E267

[3] V. Lehmann: J. Electrochem. Soc. **140** (1993) 2836

[4] E. K. Propst, P. A. Kohl: J. Electrochem. Soc. **141** (1994) 1006

[5] J, Carstensen, M. Christophersen, H. Föll: Matt. Sci. and Eng. B69-70 (2000) 23

[6] J.-N. Chazalviel, M. Etman, F. Ozanam: J. Electrochem. Chem. **297** (1991) 533

[7] R. Memming, G. Schwandt: Surf. Sci. **4** (1966) 109

[8] J. Koutecky, V. G. Levich: Dokl, Akad. Nauk. SSSR, 117 (1957): 441 Zh. Fiz. Khim. **32** (1958) 1565

[9] Yu. V. Pleskov, V. YU. Filinovskii: The Rotating Disk Electrode, Plenum Press, New York 1976, ch. 3.

[10] M. R. L. Mellier, J. E. A. M. Van den Meerakker: E. C. S. Meeting, Phoenix 2000

[11] J.-N. Chazalviel, F. Ozanam: J.Electroanal. Chem. **327** (1991) 343

[12] M. J. Eddowes: J. Electroanal. Chem. **280** (1990) 297

[13] S. Rönnebeck, J. Carstensen, S. Ottow, H. Föll: Electrochem. and Solid-State Letters, **2(3)** (1999) 126.

[14] G. S. Higashi, Y. J. Chabal, G. W. Trucks, K. Raghavachari: Appl. Phys. Lett. **56** (1990) 656

[15] V. A. Burrows, Y. J. Chabal, G. S. Higashi, K. Raghavachari, S. B. Christman: Appl. Phys. Lett. **53** (1988) 998

[16] C. da Fonseca, F. Ozanam, J.-N. Chazalviel: Surf. Sci. **365** (1996) 1-14

[17] M. Niwano: E. C. S. Meeting, Phoenix (Arizona) 2000

[18] M. Nakamura, M. B. Song, M. Ito: Electrochem. Acta **41** (1996) 681

[19] F. M. Liu, B. Ren, J-W. Yan, B-W. Mao, Z-Q. Tian: J. Electrochem. Soc. **149** (2002) G95

[20] M. Niwano: Surf. Sci. **427** (1999) 199